Effect of Ag on microstructural behaviour of Nanocrystalline $Fe_{87-x}Zr_7B_6Ag_x$ ($0 \leq x_{Ag} \leq 4$) Magnetic Thin Films Materials

W.J. Lee*,+, B.K. Min*, J.S. Song*
*Electric and Magnetic Devices Group, Korea Electrotechnology Research Institute,
Changwon 641-120, Korea

Effect of Ag additive element on microstructure of $Fe_{87-x}Zr_7B_6Ag_x$ magnetic thin films on Si(001) substrates has been investigated using Transmission Electron Microscopy(TEM) and X-ray Diffraction(XRD). All samples with additive Ag element were made by DC-sputtering and subjected to annealing treatments of 300°C ~ 600°C for 1 hr. TEM and XRD showed that perfectly amorphous state in Ag-free Fe-based films was observed in as-deposited condition. The as-deposited Fe-based films with the presence of Ag constituent have a mixture of Fe-based amorphous and nano-sized Ag crystalline phases. In this case, additive element, Ag was soluted into Fe-based matrix. With the increase in additive element, Ag, insoluble nano-crystalline Ag particles were dispersed in the Fe-based amorphous matrix. Crystallization of Fe-based amorphous phase in the matrix of $Fe_{82}Zr_7B_6Ag_5$ thin films occurred at an annealing temperature of 400℃. Upon annealing, the amorphous-Ag crystalline state of Fe-Zr-B-Ag films was transformed into the mixture of Ag crystalline phase + Fe-based amorphous phase + α-Fe cluster followed by the crystallization process of α-Fe nanocrystalline + Ag crystalline phases.

Keywords : Fe-Zr-B-Ag; Soft magnetic materials; Thin films, Nano-crystalline, TEM, XRD

1. INTRODUCTION

Nanocrystalline structure in Fe- and Co-based soft magnetic materials is crucial factor in showing low magnetic loss and high permeability at frequency ranging to GHz. Previous studies on such materials explain the contribution of nano-sized Fe or Co-base crystal precipitates existing in amorphous matrix to high frequency magnetic property improvement [1].

The improved properties are achieved in the form of small-sized magnetic domain structure by (1) the reduction of apparent magnetic anisotropy due to the accommodation of each nano-sized grain's local anisotropy [2], (2) the creation of small magnetostrictive crystalline phases [3] and (3) the increase of electrical resistivity in the presence of the phases [4].

In order to enhance magnetic property of Fe-Zr-B thin films, with several additive elements(Ti, V, Cu, Mo, Nb, Cr) have been investigated for potential uses as electrical transformers, inductors, switching supplies operating at high frequency, and other electrical devices. Here, few studies on the effect of substitution element, Ag on microstructural change in Fe-base deposited alloys for enhancing magnetic properties were carried out. Also, there is no direct observation of nano-sized Ag particles in Fe-Zr-B based amorphous matrix. Therefore, it is needed to do high resolution TEM observation on non-equilibrium Fe-base alloys produced by a DC sputtering process and alloy substitution with Ag.

This paper presents microstructural evolution of Ag-free and Fe-Zr-B-Ag film deposited on Si (100) substrate as a function of additive element, Ag ($0 \leq x_{Ag} \leq 4$), using HREM and XRD.

2. EXPERIMENTAL PROCEDURE

Ag-free $Fe_{87}Zr_7B_6$ and $Fe_{87-x}Zr_7B_6Ag_x$ thin films with 0.5 ㎛ thick were deposited from Fe-Zr-B targets and Ag chips on Si(001) substrates by using a DC-magnetron sputtering system with a base pressure of 3×10^{-6} torr and a deposition pressure 3×10^{-3} torr. The input power was 300W. Ag content in $Fe_{87-x}Zr_7B_6Ag_x$ thin films was varied by adjusting number of Ag chips and their configuration on Fe-Zr-B target. Si(001) substrates were held at 30°C during sputtering and then ex-situ annealed in vacuum furnace having a base pressure of 5×10^{-6} torr in the range of 300°C to 700°C for 1hr. X-ray diffraction (XRD) and High-resolution transmission electron microscopy (HREM) were employed for the characterization of crystal structure and microstructure of the films.

3. RESULTS AND DISCUSSION

Figure 1 shows XRD patterns of as-sputtered $Fe_{87-x}Zr_7B_6Ag_x$ thin films as a function of amount of additive element Ag. All $Fe_{87-x}Zr_7B_6Ag_x$ thin films fabricated by a sputtering method show broad XRD peaks. This

observation of amorphous peak in the XRD diffraction indicates that sputtering process was significantly effective in forming amorphous Fe-base phases in such composition.

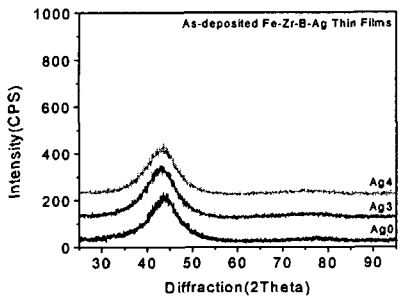

Fig. 1. XRD patterns of as-sputtered $Fe_{87-x}Zr_7B_6Ag_x$ thin films on Si(001) substrates with variation of Ag composition, x.

Also, in the case of Ag addition, central position of XRD peaks (110) in as-deposited $Fe_{87-x}Zr_7B_6Ag_x$ thin films was shifted towards the decrease in diffraction angle. As the content of Ag element into the matrix increased, the main peak in the XRD pattern much broaden. This represents that Ag additive element causes to the increase in the solubility of Fe-based matrix with increasing Ag additive, although the structure of such alloys is thermodynamically unstable. Here, main XRD peak in the case of Ag-additive $Fe_{87-x}Zr_7B_6Ag_x$ thin films was asymmetric, which represents a possibility of overlapping two peaks of Fe(110) and Ag(111). Here, a simulation for separating second peak from the main one in the XRD pattern was carried out, since the main XRD peaks were significantly asymmetric with increasing additive element, Ag. From the precise XRD analysis, we may consider the presence of crystalline peak (111) consisting of residual Ag element from the Fe-based matrix, indicating the insoluble state.

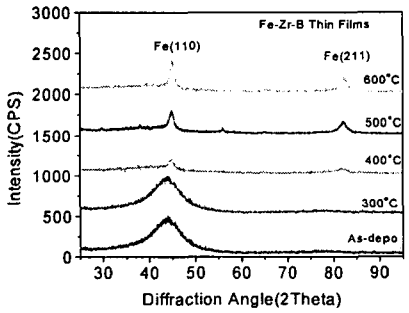

Fig. 2. XRD patterns of Ag-free $Fe_{87}Zr_7B_6$ thin films on Si(001) substrates with variation of annealing temperature.

Ag-free $Fe_{87}Zr_7B_6$ thin films experienced annealing process upto 600°C. Figure 2 shows XRD patterns of Ag-free $Fe_{87}Zr_7B_6$ thin films on Si(001) substrates with variation of annealing temperature. Below 400°C, amorphous state in $Fe_{87}Zr_7B_6$ thin films retained, but crystallization occurred at 400°C.

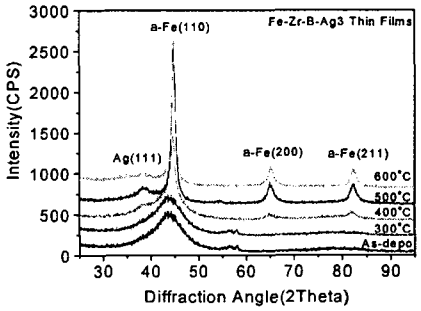

Fig.3. XRD patterns of $Fe_{84}Zr_7B_6Ag_3$ thin films with variation of annealing temperature

Figure 3 shows XRD patterns of $Fe_{84}Zr_7B_6Ag_3$ thin films with variation of annealing temperature. Main peak in the XRD patterns of as-deposited thin films was nearly symmetric. In comparison with Ag-free $Fe_{87}Zr_7B_6$ thin films, main peak in the presence of Ag was shifted towards the decrease in diffraction angle. This represents that the enhancement of solubility of Ag into Fe-base matrix of $Fe_{84}Zr_7B_6Ag_3$ thin films occurred during deposition. With increasing annealing temperature, sharp (111) peak of Ag additive element in the XRD pattern was observed. As-deposited $Fe_{84}Zr_7B_6Ag_3$ thin films were in the mixture of major Fe-based amorphous and Ag nano-sized crystalline phase. Intensity of main XRD peak(110) in α -Fe phase increased with increasing annealing temperature. Also, crystallization of the thin films occurred after annealing of the Fe-based alloys at 400°C, and XRD crystalline peaks of α -Fe and Ag phases were observed on the annealing conditions.

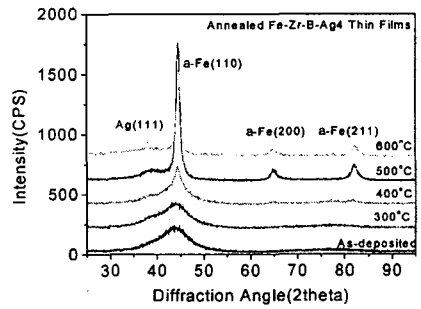

Fig.4. XRD patterns of $Fe_{83}Zr_7B_6Ag_4$ thin films with variation of annealing temperature

Figure 4 shows XRD patterns of $Fe_{83}Zr_7B_6Ag_4$ thin films with variation of annealing temperature. Main peak in the XRD patterns of as-deposited thin films was asymmetric. This represents to the occurrence of overlapping in two peaks of α -Fe(110) and Ag(111). After separation of two XRD peaks, we identified that as-deposited $Fe_{83}Zr_7B_6Ag_4$ thin films were in the mixture of major Fe-based amorphous and minor Ag crystalline phases. Intensity of main XRD peak(110) in α -Fe phase increased with increasing annealing temperature. Also, crystallization of the thin films occurred after annealing of the Fe-based alloys at 400°C, and XRD crystalline peaks of α -Fe and Ag phases were observed on the annealing conditions. Such crystallization features of all $Fe_{87-x}Zr_7B_6Ag_x$ thin films were observed in the range of Ag content, x = 0 - 4a/o. Therefore, phases transformation of as-deposited $Fe_{87-x}Zr_7B_6Ag_x$ thin films proceeded in an order of Fe-based amorphous phase + Ag crystalline phase → Fe-based amorphous phase + α -Fe cluster + Ag crystalline phase → α -Fe nano-crystalline phase + Ag crystalline phase → α -Fe crystalline phase + Ag crystalline phase.

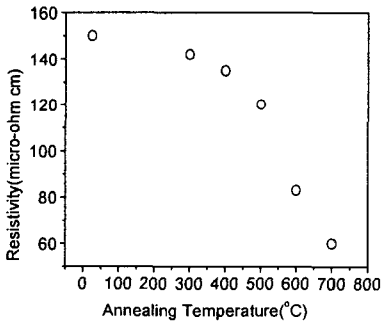

FIG.5. The change in electrical resistivity (ρ) with annealing temperature for an amorphous $Fe_{83}Zr_7B_6Ag_4$

Fig. 5 shows the change in electrical resistivity of the film with annealing temperature. The electrical resistivity of 150 μΩcm was maintained up to 400 °C, and then started to decrease linearly from 400°C with increasing the temperature. The electrical resistivity at 600°C was 80 μΩcm. As the electrical resistivity of the film at room temperature was 150 μΩcm, it was believed that the film has a typical amorphous structure. It was estimated from the change in electrical resistivity with temperature that the crystallization temperature was 400 °C.

Figure 6 shows plane-view TEM micrographs of Ag-free $Fe_{87}Zr_7B_6$ (see Fig.6a) and $Fe_{83}Zr_7B_6Ag_4$(see Fig.6b) thin films. Figure 6a shows amorphous state of as-deposited films consisting of majority of Fe-based amorphous Ag-free $Fe_{87}Zr_7B_6$. In Figure 6b, dispersion of Ag nano-sized crystalline phase was observed in the Fe-based matrix of as-deposited $Fe_{83}Zr_7B_6Ag_4$ samples. In Fig.6c, crystallization of amorphous $Fe_{83}Zr_7B_6Ag_4$ thin films occurred at 400°C and average grain size of α-Fe precipitates was about 8 nm.

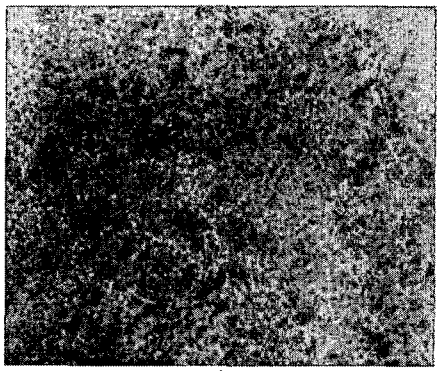

a)

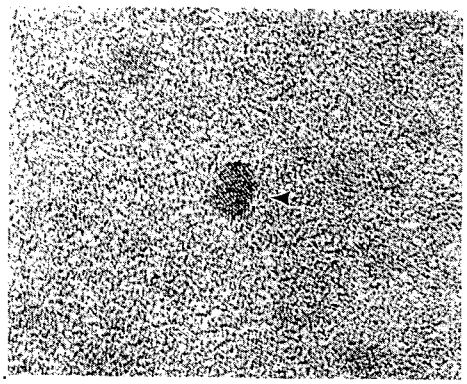

(b)

(c)

4. CONCLUSION

All samples with Ag-free and additive Ag element were made by DC-sputtering and subjected to annealing

treatments of 300°C ~ 600°C for 1 hr. HREM and XRD showed that the as-deposited Fe-based film with the presence of Ag constituent have a mixture of Fe-based amorphous and nano-sized Ag crystalline phases. In the case of Ag-free Fe-based films, perfectly amorphous state was observed in as-deposited condition. Upon annealing, the amorphous-Ag crystalline state of $Fe_{83}Zr_7B_6Ag_4$ films was transformed into the mixture of Ag crystalline phase + Fe-based amorphous phase + α-Fe cluster (at 400°C) followed by the crystallization process of α-Fe nanocrystalline + Ag crystalline phases (at 500°C) → enlarged grain α-Fe crystalline + Ag crystalline phases (at 600°C)

REFERENCES

[1] K. Suzuki, A. Makino, N. Kataoka, A. Inoue, T. Masumoto, Mater. Trans. JIM 32 (1991) 93.
[2] G. herzer, IEEE Trans. Magn. Mag-26 (1990) 1397.
[3] Y. Yoshizawa, S. Oguma and K. Yamauchi, J. Appl. Phys. 64 (1988) 6044.
[4] A. Makino and Y. Hayakawa, J. Jpn. Inst. Met. 57 (1993) 1301.
[5] W.J. Lee, B.K. Min, J.S. Song, J.S. Heo, J. MMM 232 (2001) 189.